Genova University Press – GUP
Bulletin of Environmental and Life Sciences

Issn - 2612-2960

WING SHAPE VARIATION IN *ORTHETRUM* DRAGONFLIES: FUNCTIONAL INSIGHTS FROM CITIZEN-SCIENCE IMAGES. A GEOMETRIC MORPHOMETRIC PERSPECTIVE LINKING SHAPE VARIATION AND SPECIES IDENTITY

MATTEO ZINNI[1,*], CLAUDIO BELLANTUONI[2], SARA FERRANDO[2], FEDERICO MAGGIOLO[2], LORIS GALLI[2]

[1] Agricolture Biodiverisity and Technologies (Abit) S.r.l., Milan, Italy.
[2] Department of Earth, Environmental and Life Sciences (DISTAV), University of Genova, Corso Europa 26, 16132 Genova, Italy.

*Correspondence: matteo.zinni@abit-agritech.com

ABSTRACT

Wing morphology in dragonflies reflects a complex interplay of functional constraints, ecological adaptation, and sexual dimorphism. Using landmark-based geometric morphometrics on fore- and hindwings of multiple *Orthetrum* species, we quantified interspecific and intraspecific variation, assessed sexual shape differences, and evaluated the contribution of allometry to observed patterns. Hindwing morphology consistently captured stronger and more structured interspecific signals than forewings, with variation concentrated in functionally relevant regions such as the wing base and anal lobe. Sexual dimorphism was detectable but weaker, primarily expressed in hindwings, while forewing shape appeared constrained by stabilizing functional requirements. Allometric effects modulated but did not hide species-specific shape divergence. Notably, high-quality digital images sourced from iNaturalist have proven suitable for large-scale morphometric analyses, enabling broad geographic and taxonomic coverage. Our results highlight the potential of hindwing morphology as a tool for species discrimination and provide a framework for integrating ecological, behavioral, and genetic data to understand the drivers of wing shape evolution in Odonata.

KEY-WORDS: Dragonflies, DragonflyPix, iNaturalist, Libellulidae, wing morphology.

INTRODUCTION

The order *Odonata*, comprising dragonflies and damselflies, has long been recognized as a valuable model group for evolutionary, ecological, and taxonomic research due to its wide geographic distribution, ecological sensitivity, and well-documented life-history traits (Corbet, 1999; Dijkstra et al., 2013). Odonates display remarkable morphological diversity and ecological specialization, making them ideal for studies requiring fine-scale taxonomic resolution. However, traditional taxonomy based solely on external morphology has often proved insufficient to resolve species boundaries within the group, particularly in genera characterized by cryptic speciation, subtle diagnostic traits, and high intraspecific variability (Dumont et al., 2010). The genus *Orthetrum*, within the diverse family Libellulidae, well exemplifies these taxonomic challenges. Widely distributed across tropical and subtropical regions of the Old World, this genus currently includes more than 60 described species (Silsby, 2001), many of which are morphologically similar and exhibit overlapping geographic ranges. Nevertheless, the family Libellulidae as a whole includes multiple recognized species complexes (Marinov, 2001; Yong et al., 2014), further contributing to the difficulty of achieving consistent and reliable species delimitation. As a

result, misidentifications are frequent, and several unresolved species complexes continue to complicate systematic efforts (Dijkstra & Kalkman, 2012). Among the anatomical structures traditionally used in odonate taxonomy, wings occupy a central role. Their intricate venation pattern - unique to Odonata - is functionally linked to aerodynamic performance, mechanical resistance, and flight efficiency (Wootton, 1991). As wing shape emerges from the interplay between developmental constraints and ecological selection pressures (Johansson et al., 2009), it often encodes subtle yet informative morphological differences among closely related taxa. This makes wing morphology particularly suitable for quantitative approaches capable of capturing fine-scale variation. Within this framework, geometric morphometrics (GM) provides a powerful analytical tool for dissecting shape differences in a statistically rigorous manner. By quantifying the spatial configuration of homologous wing landmarks, this method allows us to detect interspecific divergence and intraspecific variability that may remain overlooked using traditional qualitative assessments. In Odonata, GM has been successfully applied to differentiate closely related species and even populations, particularly using wing venation patterns, which are highly species-specific and relatively stable within individuals (Outomuro & Johansson, 2011). For taxonomically challenging groups such as the genus *Orthetrum*, wing shape analysis through geometric morphometrics offers a promising avenue for improving taxonomic resolution. Consequently, applying this approach to *Orthetrum* wings not only contributes to a clearer understanding of morphological differentiation within the genus but also provides a replicable framework for supporting species delimitation in odonates more broadly. In recent years, the growing availability of high-quality digital photographs from natural history collections, online repositories, and citizen science platforms such as iNaturalist (https://www.inaturalist.org) has opened new opportunities for large-scale morphometric research. These sources greatly expand the spatial and temporal coverage of sampling, enabling the inclusion of specimens from regions that would otherwise be logistically inaccessible or underrepresented in field collections (Mason et al, 2025). Although images acquired under non-standardized conditions can introduce sources of variation, several studies have demonstrated that geometric morphometrics is robust to moderate differences in image quality, angle, and lighting when homologous structures such as wing venation are clearly visible (Cardini et al., 2022; Fox et al., 2020). The use of curated online archives therefore represents a valuable complement to traditional specimen-based datasets. In this study, we leverage these digital resources to analyse forewing and hindwing shape variation across *Orthetrum* species, demonstrating how community-generated data can effectively support taxonomic and morphological investigations in Odonata. Given the taxonomic complexity of the genus *Orthetrum* and the demonstrated potential of wing geometric morphometrics to capture subtle shape variation, the present study aims to evaluate the effectiveness of forewing and hindwing shape analysis as tools for improving species delimitation within this group. Specifically, we (i) quantify interspecific differences in hindwing morphology across a representative subset of *Orthetrum* species using landmark-based geometric morphometrics; (ii) assess the magnitude of intraspecific variation relative to interspecific divergence to determine the taxonomic resolution achievable through wing shape; (iii) examine sexual shape dimorphism to evaluate whether males and females exhibit consistent and detectable morphological differences in wing configuration; and (iv) test the feasibility and reliability of using digital images sourced from iNaturalist and other online repositories as a data source for large-scale morphometric

analyses. By combining traditional morphometric rigor with community-generated imagery, this study provides a scalable framework for morphological investigations in Odonata and contributes to a deeper understanding of shape diversification within *Orthetrum*.

MATERIALS AND METHODS

Data preparation - Shape and size variations in the forewings and hindwings of 10 Anisoptera species belonging to the family *Libellulidae* were analyzed using landmark-based geometric morphometrics (Bookstein, 1997; Adams et al., 2004). A total of 120 wing images were selected from nine species of the genus *Orthetrum* (*O. albistylum*, *O. brunneum*, *O. cancellatum*, *O. coerulescens*, *O. glaucum*, *O. julia*, *O. pruinosum*, *O. sabina*, *O. taeniolatum*, *O. trinacria*) and one species of the genus *Libellula* (*L. depressa*) (Table 1). *Libellula depressa* was included as an external outgroup-like reference taxon to provide a broader morphological context for interpreting shape variation within the genus *Orthetrum* without being directly involved in the focal taxonomic comparisons but concurrently calibrate the overall range of morphological variation, verify the robustness of landmarking and Procrustes alignment on a more divergent wing shape, and provide a comparative benchmark for interpreting dispersion and group separation within multivariate analysis. Images were obtained from three open-access repositories: the Data Portal of the Natural History Museum (London, UK; https://data.nhm.ac.uk/), iNaturalist, and DragonflyPix (https://www.dragonflypix.com/). The correspondence between image records and taxonomic assignments was verified by the authors. For iNaturalist, only records classified as "research grade" (highest data reliability level) were included. Specimens were selected based on the criterion that both forewings and hindwings were positioned in a coplanar arrangement, with all veins and nodal intersections in focus on the same plane. Geometric morphometric data were processed using *tpsUtil* (v. 1.74; Rohlf, 2017a) for image management and *tpsDig* (v. 2.30; Rohlf, 2017b) for landmark digitization. Landmarks represented homologous anatomical loci (Zelditch et al., 2012) and were chosen based on consistent, reproducible anatomical features across all examined species. A total of 20 type I landmarks were placed on each forewing and 22 on each hindwing (Table 2, Figure 1). Landmarks were located at intersections of major veins with the wing margin, branch points, and junctions of transverse and longitudinal veins, following established morphological criteria for Odonata (Huang et al., 2020). Digitization of forewing and hindwing landmarks was conducted separately to minimize measurement error, prevent artifacts mainly resulting from the different mutual position of the two wings, and allow a more precise comparison of shape and size variation. Before the Generalized Procrustes Analysis (GPA), all landmark configurations were mirrored so that all wings were oriented as left wings, preventing unwanted inversions during superimposition. Landmark configurations were then aligned using GPA (Gower, 1975; Rohlf & Slice, 1990), which removes non-shape variation by translating, scaling, and rotating specimens to achieve optimal alignment. The centroid size (CS) was computed as the square root of the summed squared distances of all landmarks from their centroid, providing a measure of overall wing size. The resulting Procrustes shape coordinates represent orthogonal projections in Kendall's tangent space (Dryden & Mardia, 1998; Rohlf, 1999) and were used for subsequent analyses. Before proceeding with multivariate analyses, the dataset was inspected for potential

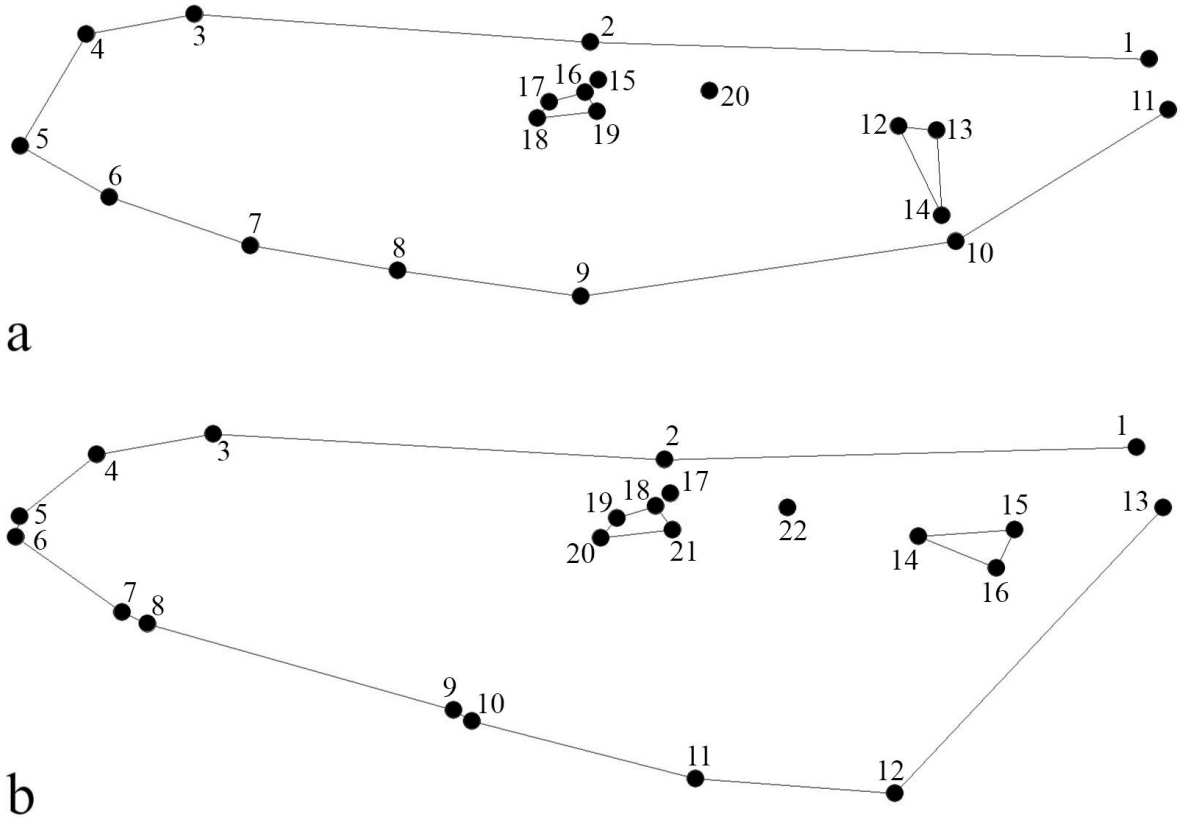

Figure 1. The positions and the numbering of the landmarks used for the study of forewing (a) and hindwing (b).

outliers related to either species or sex using the *plotOutliers* function. Two additional reduced datasets were thus generated, from which specimens exceeding the percentage were excluded. After outlier removal, landmark configurations were re-aligned through a second Generalized Procrustes Analysis to preserve shape consistency across datasets. Given the unbalanced nature of the data, the effects of taxonomy and sex on wing shape were investigated separately to improve statistical power and avoid confounding due to underrepresented species–sex combinations. Analyses were therefore performed on both the complete and reduced datasets, allowing the evaluation of morphological trends under increasingly controlled conditions and ensuring that observed shape variation reflected genuine biological differences rather than artefacts due to atypical individuals or sampling imbalance. All analyses were conducted in R (v. 4.3.0) using the packages *geomorph* (Baken et al., 2021), *RRPP* (Collyer & Adams, 2018), *MASS* (Ripley et al., 2013), and *Morpho* (Schlager et al., 2019).

Allometry - Allometric effects were investigated to evaluate the potential influence of size variation on wing shape in both forewings and hindwings. Centroid size (CS) was used as a proxy for overall wing size. The distribution of CS values was examined to assess interspecific and intersexual differences, since size heterogeneity may influence the estimation of shape variation. The Kruskal-Wallis test was employed to test the null hypothesis of equal CS distributions among groups, and Dunn's test was used for post-hoc pairwise comparisons whenever significant differences were detected. The relationship between wing shape and size was then investigated by

Table 1. Number of individuals digitized for forewing and hindwing, reported separately for males and females for each species; total sample size per species is indicated.

	Forewing		**Total**	**Hindwing**		**Total**
Species	**Male**	**Female**		**Male**	**Female**	
Orthetrum albistylum	8	4	12	8	4	12
Orthetrum brunneum	8	4	12	8	4	12
Orthetrum cancellatum	7	5	12	7	5	12
Orthetrum coerulescens	4	8	12	4	8	12
Orthetrum glaucum	6	6	12	6	6	12
Orthetrum julia	5	7	12	5	7	12
Orthetrum pruinosum	10	2	12	10	2	12
Orthetrum sabina	6	6	12	6	6	12
Orthetrum trinacria	8	4	12	8	4	12
Libellula depressa	6	6	12	6	6	12

Table 2. Description and numbering of the selected landmarks for forewing (left) and hindwing (right).

Forewing	**Definition**	**Hindwing**	**Definition**
1	Initial of costa	1	Initial of costa
2	Nodus	2	Nodus
3	Left of stigma	3	Left of stigma
4	Right of stigma	4	Right of stigma
5	Midpoint of 4 and 6	5	End of Sub-costa
6	End of RP2	6	End of RP1
7	Midpoint of 6 and 8	7	End of RP2
8	End of RP3-4	8	End of IRP2
9 - 10	Anal region	9	End of RP3-4
11	End of the anal vein	10	End of MA
12, 13, 14	Triangle region	11	End of CuP
15	Sub-nodus	12	Anal region
16, 17,18, 19,20	Midvein region	13	End of the anal vein
		14, 15, 16	Triangle region
		17	Sub-nodu
		18, 19, 20, 21, 25	Midvein region

means of multivariate regressions of Procrustes-aligned coordinates on the logarithm of centroid size. This approach quantifies the proportion of shape variation explained by size and tests its statistical significance using permutation procedures (9999 iterations). To account for potential differences in allometric trajectories among groups, two alternative models were compared: one assuming a common slope (shared allometric pattern) and another allowing group-specific slopes. Pairwise comparisons among groups were further used to examine differences in the direction and magnitude of allometric vectors.

To assess whether the magnitude of size-shape relationships differed among species, species-specific allometric slopes obtained from multivariate regressions of wing shape on centroid size were compared. For each species, the regression slope was expressed as a vector describing shape change per unit increase in size. The length of the slope vector was used as a measure of the strength of allometry. Pairwise comparisons of species-specific allometric slopes were performed using the *pairwise* function from the RRPP package, considering three complementary metrics to quantify differences among slopes: DL (difference in vector lengths), the absolute difference in slope vector lengths reflecting variation in the magnitude of allometric shape change per unit size; dist (distance between vectors), the Euclidean distance between slope vector endpoints summarizing overall differences in multivariate trajectories; and VC (vector correlation), the correlation between slope vectors scaled to unit length, with angles (expressed as arccos) describing divergence in trajectory orientation independent of magnitude. Statistical significance of pairwise differences was assessed using 9999 RRPP permutations. All mentioned analyses were conducted separately for forewings and hindwings and repeated on both the complete and reduced datasets described above, ensuring that the assessment of size-shape relationships was not affected by atypical observations.

Shape analysis - Principal component analysis (PCA) was applied to the procrustes-aligned landmark coordinates of the full datasets to characterize the overall structure of wing shape variation (Klingenberg & McIntyre, 1998; Klingenberg & Zaklan, 2000). PCA decomposes the covariance matrix of the shape variables into orthogonal axes called principal components (PCs) ordered by decreasing variance, thereby providing a low-dimensional representation of the high-dimensional procrustes coordinates. PCA scores were used to visualize morphospace occupancy at both individual and species levels for forewing and hindwing. Shape changes associated with the main PCs were illustrated using vector displacement plots, which allow us to depict landmark displacements from the mean shape toward the extremes of each axis and provide a qualitative assessment of dominant directions of morphological variation. PCA was conducted on the full dataset to represent the total morphological variation across species and sexes. Since allometric regressions are more sensitive to extreme values, allometry was evaluated on reduced datasets from which species-level or sex-related outliers were removed.

Additional PCAs were however conducted on reduced datasets in which species-level or sex-related outliers had been removed. Canonical variate analysis (CVA) was used to find the shape features that best distinguish among multiple groups of specimens (Gumiel et al., 2003, Villemant et al., 2007). In CVA, groups membership is treated as known a priori, and the analysis was used to test whether wing shape variation observed through GPA and PCA reflects biologically meaningful differences among these groups. For each dataset (full dataset, dataset without species outliers, dataset without sex outliers), CVA was performed with leave-one-out cross-validation and with 9999 permutations to assess the statistical significance of group separation.

Loadings and other data and results used in the analyses are reported in the supplementary materials (Tables S1 to S13).

RESULTS

Data preparation - In total, 14 unique forewing specimens and 13 unique hindwing specimens were classified as outliers across all analyses. For forewings, 6 outliers were identified across species and 8 across sexes, with some specimens overlapping between these groups. In hindwings, 9 outliers were detected across species and seven across sexes, with partial overlap between groups. These outlier specimens were retained for subsequent morphometric analyses to evaluate their potential influence on wing shape.

For forewings, centroid size differed significantly among species (Kruskal-Wallis $\chi^2 = 34.64$, $df = 9$, $p < 0.01$) but not between sexes ($\chi^2 = 0.03$, $df = 1$, $p > 0.05$). Post-hoc comparisons indicated that a few species, particularly *O. julia*, showed significant differences from others, while most species pairs did not differ significantly after Bonferroni correction. For hindwings, centroid size also varied significantly among species ($\chi^2 = 36.18$, $df = 9$, $p < 0.01$), with no significant differences between sexes ($\chi^2 = 0.21$, $df = 1$, $p > 0.05$). Similarly, post-hoc tests highlighted that a limited number of species, especially *O. julia*, differed significantly from the others. Analyses conducted after removing species-specific outliers showed that interspecific differences in centroid size remained significant for both forewings ($\chi^2 = 33.38$, $df = 9$, $p < 0.01$) and hindwings ($\chi^2 = 35.63$, $df = 9$, $p < 0.01$). Removing sex-specific outliers did not affect the absence of significant sexual dimorphism in either forewings ($\chi^2 = 0.10$, $df = 1$, $p > 0.05$) or hindwings ($\chi^2 = 0.02$, $df = 1$, $p > 0.05$).

Allometry - The effect of size on forewing shape was assessed using Procrustes-based multivariate regression. For the full dataset, several models were compared: a null model, a simple size-on-shape model, a common-slope model, and a unique-slope model based on the interaction between the size element and the species. Model selection based on permutation ANOVA indicated that the unique-slope model best explained the data related to the forewing ($R^2 = 0.30$, $p < 0.01$, Table 3), highlighting heterogeneous allometric trajectories among species. When species outliers were removed, the unique-slope model again provided the best fit ($R^2 = 0.34$, $p < 0.01$). Following pairwise comparisons of slope vectors revealed that most species differed in slope direction or magnitude, although some pairs had overlapping confidence intervals, suggesting partially shared allometric patterns (Tables S1 to S3). For the hindwing among the models tested, the unique-slope model provided the best fit, both in the full dataset ($R^2 = 0.29$, $p < 0.01$, Table 4) and in the dataset with species outliers removed ($R^2 = 0.34$, $p < 0.01$), indicating species-specific allometric trajectories. The common-slope model was also significant in both datasets ($R^2 = 0.23–0.27$, $p < 0.01$) but less explanatory (Table 4), confirming that species differ in both the magnitude and direction of allometric shape change. Pairwise comparisons of species-specific allometric slopes for the forewing showed that interspecific differences in the magnitude and orientation of allometric trajectories were somehow dissimilar but generally limited. Differences in slope vector lengths (DL, Table S1) were small for most species pairs (0.001–0.13), with effect sizes mostly below $Z = 2$ and non-significant ($p > 0.05$), indicating broadly comparable rates of shape change per unit increase in size. Although the distances between slope vectors (dist) were low to moderate (0.03–0.20; $Z < 2.5$ for most comparisons), suggesting that the overall amount of multivariate shape change is similar between species, the couples *albistylum* - *julia* ($p \leq 0.05$), *coerulescens* - *julia* ($p \leq 0.05$), *glaucum* - *julia* ($p \leq 0.05$), *julia* - *pruinosum* ($p \leq 0.001$) and *julia* - *trinacria* ($p < 0.01$) showed significant structured

differences (Table S2). Vector correlations (VC, Table S3) ranged from strongly negative to moderately positive, with angles between vectors mostly large, yet only a few species pairs - particularly those involving *O. Julia* - showed significant divergence in trajectory orientation (Z up to 2.73; $p < 0.05$). Hindwing allometric trajectories were largely conserved across *Orthetrum* species, showing limited interspecific variation in both magnitude and direction of shape change. DL analysis revealed minimal differences in slope lengths, ranging from 0.0005 to 0.2372, with low effect sizes (Z) and all pairwise P-values > 0.05 (Table S4), indicating broadly similar rates of shape change per unit increase in size. Distance (Dist) comparisons confirmed these patterns: pairwise distances between trajectory end-points varied moderately (0.036–0.237) but were not statistically significant, suggesting a shared allometric pattern. *Orthetrum cancellatum* exhibited slightly higher distances relative to most other species, while *albistylum*, *coerulescens*, *glaucum*, and *pruinosum* displayed very small differences (Table S5), highlighting high similarity. Vector Correlation (VC) analysis showed that the directions of allometric vectors were not strictly parallel, with correlation coefficients between -0.6328 and 0.7036. Only *coerulescens* versus *trinacria* differed significantly ($p < 0.05$, Table S6), and effect sizes (Z) were generally moderate (-1.3025 to 1.7864). Overall, these results indicate that, despite slight interspecific divergence, the general direction and magnitude of hindwing shape change with size are broadly similar across species. Sex had a statistically significant effect both in determining forewing ($R^2 = 0.06$, $p < 0.01$) and hindwing ($R^2 = 0.07$, $F = 4.40$, $P < 0.01$) allometries, but its contribution to shape variation was negligible and is therefore not considered further.

Table 3. Forewing allometry - ANOVA table used to select the best model within fitted candidates in the reduced dataset without species outliers.

Model	**ResDf**	**Df**	**RSS**	**SS**	**MS**	**R²**	**F**	**Z**	**Pr(>F)**
Shape ~ 1 (Null)	107	1	0.23						
Shape ~ log(CS)	106	1	0.23	0.01	0.01	0.02	2.40	1.94	0.03
Shape ~ log(CS) * Species	88	19	0.15	0.08	0.00	0.34	2.35	5.19	<0.01
Shape ~ log(CS) + Species	97	10	0.17	0.06	0.01	0.26	3.41	6.88	<0.01
Total	107		0.23						

Table 4. Hindwing allometry - ANOVA table used to select the best model within fitted candidates in the reduced dataset without species outliers.

Model	**ResDf**	**Df**	**RSS**	**SS**	**MS**	**R²**	**F**	**Z**	**Pr(>F)**
Shape ~ 1 (Null)	110	1	0.30						
Shape ~ log(CS)	109	1	0.29	0.01	0.01	0.03	3.48	2.13	0.01
Shape ~ log(CS) * Species	91	19	0.20	0.10	0.01	0.34	2.42	4.82	<0.01
Shape ~ log(CS) + Species	100	10	0.22	0.08	0.01	0.27	3.79	5.81	<0.01
Total	110		0.30						

Shape analysis - PCA was first performed on the full dataset to describe the overall structure of forewing and hindwing shape variation. Additional PCAs were conducted after removing species-level and sex-related outliers to assess the robustness of the major axes of variation. These sensitivity analyses produced qualitatively similar ordinations and did not alter the main biological interpretation; therefore, the PCA based on the full dataset is presented as the

primary analysis. For forewings, the first two principal components accounted for 51.60% of total shape variance (PC1: 30.66%; PC2: 20.93%). The third component (PC3) explained a further 8.97% of variance, bringing the cumulative proportion of explained variation for the first three PCs to 60.6%. The first principal axis was mainly driven by landmarks related to posterior margin (LM8, LM9, LM7, Table S7) followed by costal and costal-distal (LM2, LM3 and LM4) landmarks that contribute with a lower magnitude in the opposite direction, reflecting a distal-proximal gradient of forewing shape (Figure 2). The second principal axis involved primarily posterior and anal landmarks, with distal-posterior landmarks (LM7, LM9, LM8) showing again positive loadings with other distal elements (LM4, LM6) negative loadings, representing variation along the posterior margin and a contraction of the wing tip (Table S8, Figure 2). The third principal axes captured localized variation in central and proximal regions, with positive loadings on central proximal landmarks (LM11, Table S9) and negative loadings near the nodus and central region (LM17–LM18 and LM19), reflecting subtle torsional and positional shifts (Figure 2). The scoreplot of individual observations in the translated morphospace along the first three principal components showed a clear trend along PC1. Females tended to have predominantly negative scores (mean ± SD: -0.012 ± 0.028), whereas males generally showed positive scores (0.008 ± 0.031). In contrast, PC2 and PC3 did not display consistent differences between sexes. For PC2, females had a mean ± SD of 0.004 ± 0.022, and males 0.003 ± 0.024. Similarly, PC3 scores were close between sexes (females 0.002 ± 0.017, males 0.001 ± 0.018). Kruskal-Wallis tests confirmed these observations: scores along PC1 differed significantly between sexes (χ^2 = 25.15, df = 1, $p < 0.01$), whereas PC2 and PC3 showed no significant sexual differences (PC2: χ^2 = 0.23, $p = 0.63$; PC3: $\chi^2 = 3.22$, $p > 0.05$). Nevertheless, Kruskal-Wallis tests revealed significant differences among species along all three PCs. Post hoc pairwise comparisons highlighted a few specific contrasts, such as *O. coerulescens* vs *O. cancellatum* on PC1, *O. coerulescens* vs *O. albistylum*, *O. brunneum*, and *O. cancellatum* on PC2, and *O. glaucum* vs multiple species on PC3. Principal component analysis (PCA) of hindwing shape data revealed that most of the variation was concentrated in the first few axes. The first principal component alone accounted for 50.82% of total shape variation, indicating a dominant axis of morphological variability within the dataset. PC2 explained an additional 22.33%, bringing the cumulative proportion of explained variance to 73.16% for the first two components (Figure 3). Analysis of the PC1 loadings (Table S10) revealed a highly structured pattern of covariation across the hindwing. The landmarks showing the largest displacement magnitudes were located primarily along the distal and posterodistal wing margin (LM9–LM11), with magnitudes ranging from 0.39 to 0.41, making this region the dominant contributor to the first principal component (Figure 2). A second group of influencing loadings occurred at the proximal and anteroproximal region of the hindwing (LM3–LM4), which exhibited strong negative values and high displacement magnitudes (0.26–0.33) occurring along a rather short portion corresponding to pterostigmatic region. This indicates coordinated variation in basal width and the configuration of the proximal anal field, contributing to changes in the overall aspect ratio of the wing. Loadings related to PC2 indicated that variation was dominated by landmarks located along the distal and posterodistal margin of the hindwing (Figure 2, Table S11). LM11 showed the highest displacement magnitude (0.46), followed by LM9–LM10 (0.38–0.37) and LM12 (0.35). These loadings describe strong covariation

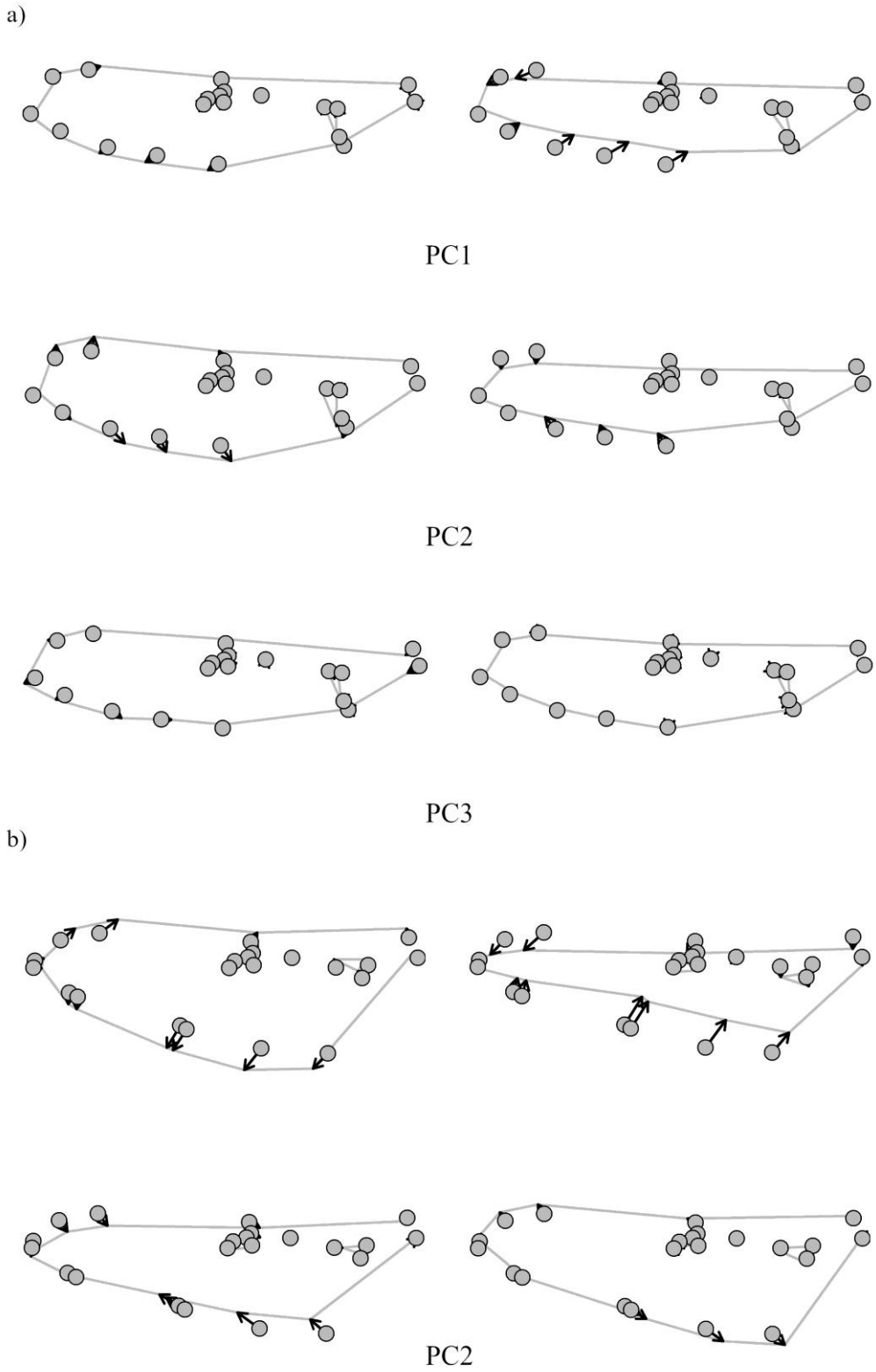

Figure 2. Vector deformation plots showing shape changes in the forewing (a) and hindwing (b) of *Orthetrum* along the main axis of variation identified by the PCA. Deformation vectors represent landmark displacements from the mean shape toward the extreme negative (left) and positive (right) of the selected principal component.

in the geometry of the posterior - proximal wing contour. A second cluster of relatively high magnitudes was observed at LM3–LM4 (0.25–0.23), suggesting additional variation in the very proximal portion of the wing as observed for PC1. Kruskal-Wallis tests indicated that hindwing shape differed significantly between sexes along the first two principal components. PC1 scores showed a significant difference between males and females ($\chi^2 = 6.52$, df = 1, $p < 0.05$), while the difference was even more pronounced for PC2 scores ($\chi^2 = 14.22$, df = 1, $p < 0.001$). These results suggest that both the primary axis of variation (PC1) and the secondary axis (PC2) are associated with sexual dimorphism in hindwing morphology (Figure 4). Pairwise comparisons following the significant Kruskal-Wallis test showed that most species pairs did not differ significantly. Relevant differences were detected for comparisons involving mostly *L. depressa*: specifically, *L. depressa* differed from *O. cancellatum* ($p < 0.01$), from *O. glaucum* ($p < 0.05$), from *O. julia* ($p < 0.05$), from *O. pruinosum* ($p < 0.05$), and from *O. sabina* ($p < 0.01$). No other pair of species showed statistically significant differences.

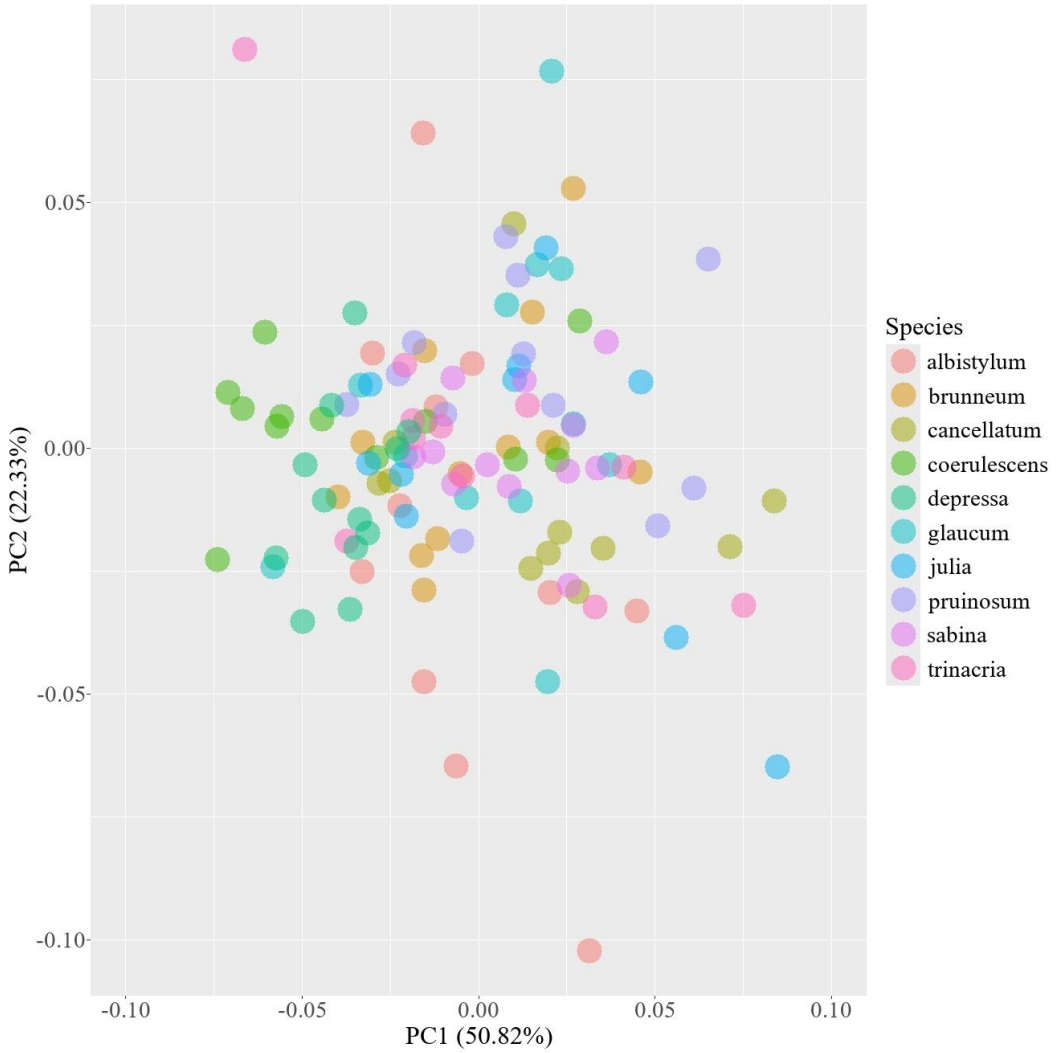

Figure 3. PCA score plot of hindwing shape in the genus *Orthetrum* (+ *Libellula depressa*) based on landmark coordinates after Generalized Procrustes Analysis. PC1 and PC2 explain 50.82% and 22.33% of total shape variation, respectively. Each point represents an individual; colours indicate species.

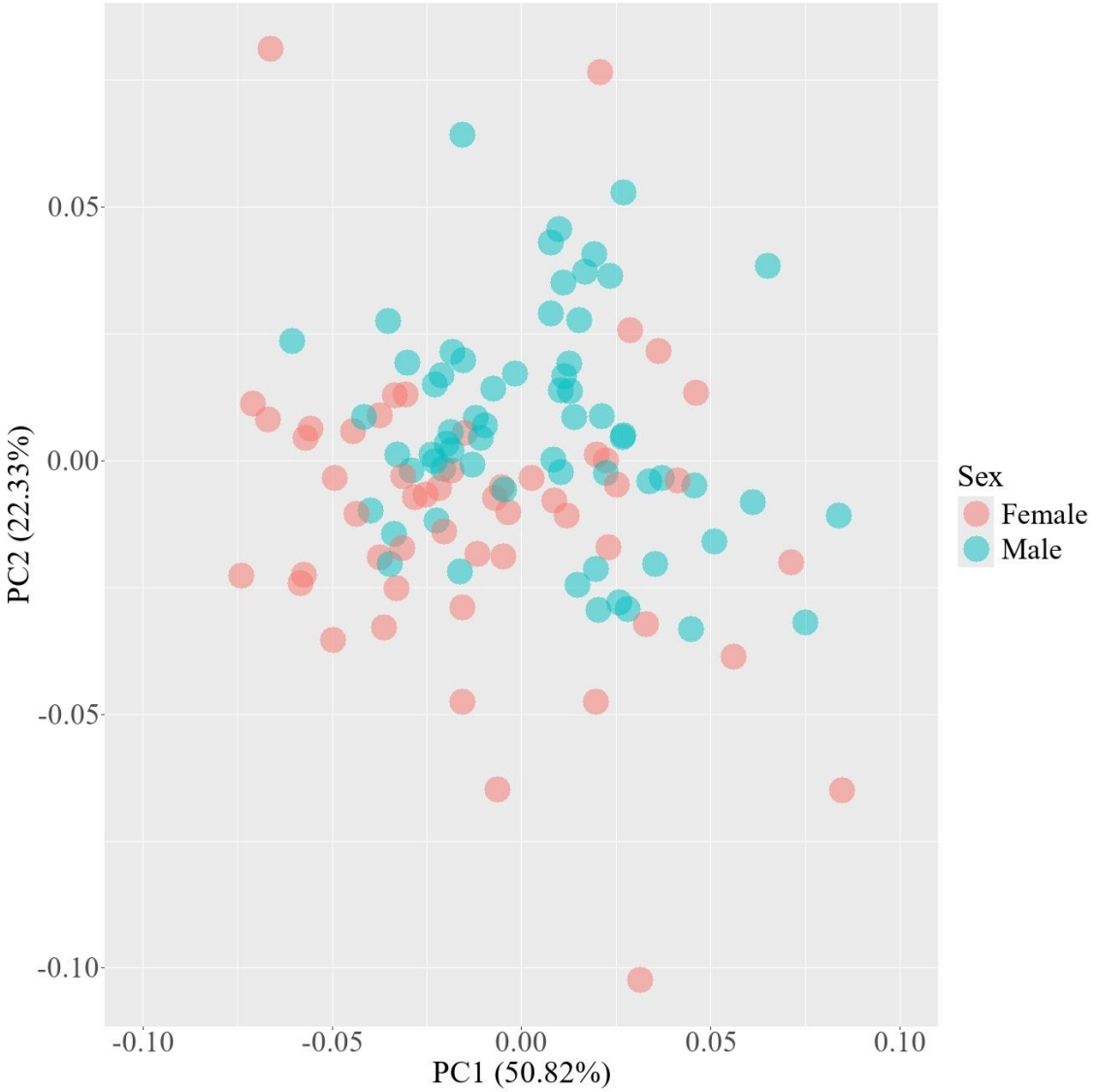

Figure 4. PCA score-plot of hindwing shape in *Orthetrum* (+ *Libellula depressa*). Each point represents an individual; colours indicate sex.

Canonical Variate Analysis (CVA) performed on forewing landmark configurations showed a clear morphological separation among the ten species. The first canonical variate accounted for 43.5% of the total among-group variation, while CV2 and CV3 explained an additional 18.4% and 14.7%, respectively. Cross-validated classification yielded an overall accuracy of 74.2%, with a Cohen's κ = 0.71, indicating substantial discriminative power of forewing shape. Classification success varied across species (Table 5): *O. coerulescens* and *L. depressa* were perfectly identified (100% correct classification), while *O. cancellatum*, *O. pruinosum*, and *O. trinacria* also showed high assignment accuracy (83.3%, 91.7%, and 75.0%, respectively). In contrast, misclassification was more frequent among *O. albistylum*, *O. brunneum*, *O. glaucum*, *O. julia*, and *O. sabina*. These species exhibited partial overlap in the shape space of the forewing, consistent with their cross-validated confusion matrices. Notably, *O.*

glaucum displayed pronounced ambiguity, with only 50% of individuals correctly classified, and substantial misassignment toward *O. julia* and *O. pruinosum*. Similarly, *O. sabina* showed moderate cross-classification with *O. trinacria* (33.3%). Conversely, species pairs such as *O. coerulescens* - *L. depressa* and *O. cancellatum* - *O. coerulescens* were completely discriminated in the CVA space. Pairwise Mahalanobis distances revealed clear and statistically significant differences in forewing shape among almost all *Orthetrum* species (Table S12). Distances ranged from moderate to high, with most comparisons showing $p < 0.01$. The smallest separation occurred between *O. sabina* and *O. trinacria* (MD = 4.28, $p < 0.05$), the only pair not remaining significant under strict correction. Other relatively close pairs

Table 5. Cross-validated classification matrix (%) obtained from Canonical Variate Analysis (CVA) of Procrustes-aligned forewing landmark data. Species abbreviations: alb (*albistylum*), bru (*brunneum*), can (*cancellatum*), coe (*coerulescens*), dep (*depressa*), gla (*glaucum*), jul (*julia*), pru (*pruinosum*), sab (*sabina*), tri (*trinacria*).

	alb	**bru**	**can**	**coe**	**dep**	**gla**	**jul**	**pru**	**sab**	**tri**
alb	58.33	8.33	25.00	0.00	0.00	0.00	0.00	8.33	0.00	0.00
bru	0.00	58.33	25.00	8.33	0.00	0.00	8.33	0.00	0.00	0.00
can	8.33	8.33	83.33	0.00	0.00	0.00	0.00	0.00	0.00	0.00
coe	0.00	0.00	0.00	100.00	0.00	0.00	0.00	0.00	0.00	0.00
dep	0.00	0.00	0.00	0.00	100.00	0.00	0.00	0.00	0.00	0.00
gla	0.00	0.00	0.00	0.00	0.00	50.00	25.00	25.00	0.00	0.00
jul	8.33	0.00	0.00	0.00	0.00	16.67	58.33	0.00	0.00	16.67
pru	0.00	8.33	0.00	0.00	0.00	0.00	0.00	91.67	0.00	0.00
sab	0.00	0.00	0.00	0.00	0.00	0.00	0.00	0.00	66.67	33.33
tri	0.00	0.00	8.33	0.00	0.00	0.00	0.00	0.00	16.67	75.00

involved *O. glaucum*, *O. julia*, and *O. pruinosum*, consistent with their partial overlap in the CVA classification. Linear discriminant analysis (LDA) was conducted to test for sexual differences in forewing shape: males and females were significantly differentiated in shape (Mahalanobis distance = 2.63, $p < 0.01$). Cross-validated classification correctly assigned 75% of individuals to their sex, with a Cohen's κ of 0.48, indicating moderate discriminative power. Classification was more accurate for males (82.4%) than for females (65.4%), reflecting partial overlap in forewing shape between sexes. Overall, these results demonstrate statistically significant sexual dimorphism in forewing morphology, though the differences are moderate. Classification performed on hindwing landmark data depicted a clear morphological separation among the ten libellulid species (Figure 5). The first canonical variate accounted for 34.8% of the total variation, with CV2 and CV3 adding to this value 20.8% and 17.3%, respectively. Together, the first three variates captured 72.9% of the discriminatory signal in hindwing shape. The classification following the cross validation assigned 76.7% of individuals to their species correctly (Table 6), with a Cohen's κ of 0.74. While some species such as *L. depressa*, *O. sabina*, *O. coerulescens*, and *O. trinacria* were almost perfectly classified, *O. albistylum*, *O. brunneum*, *O. cancellatum*, *O. glaucum*, *O. julia*, and *O. pruinosum* showed partial misclassification,

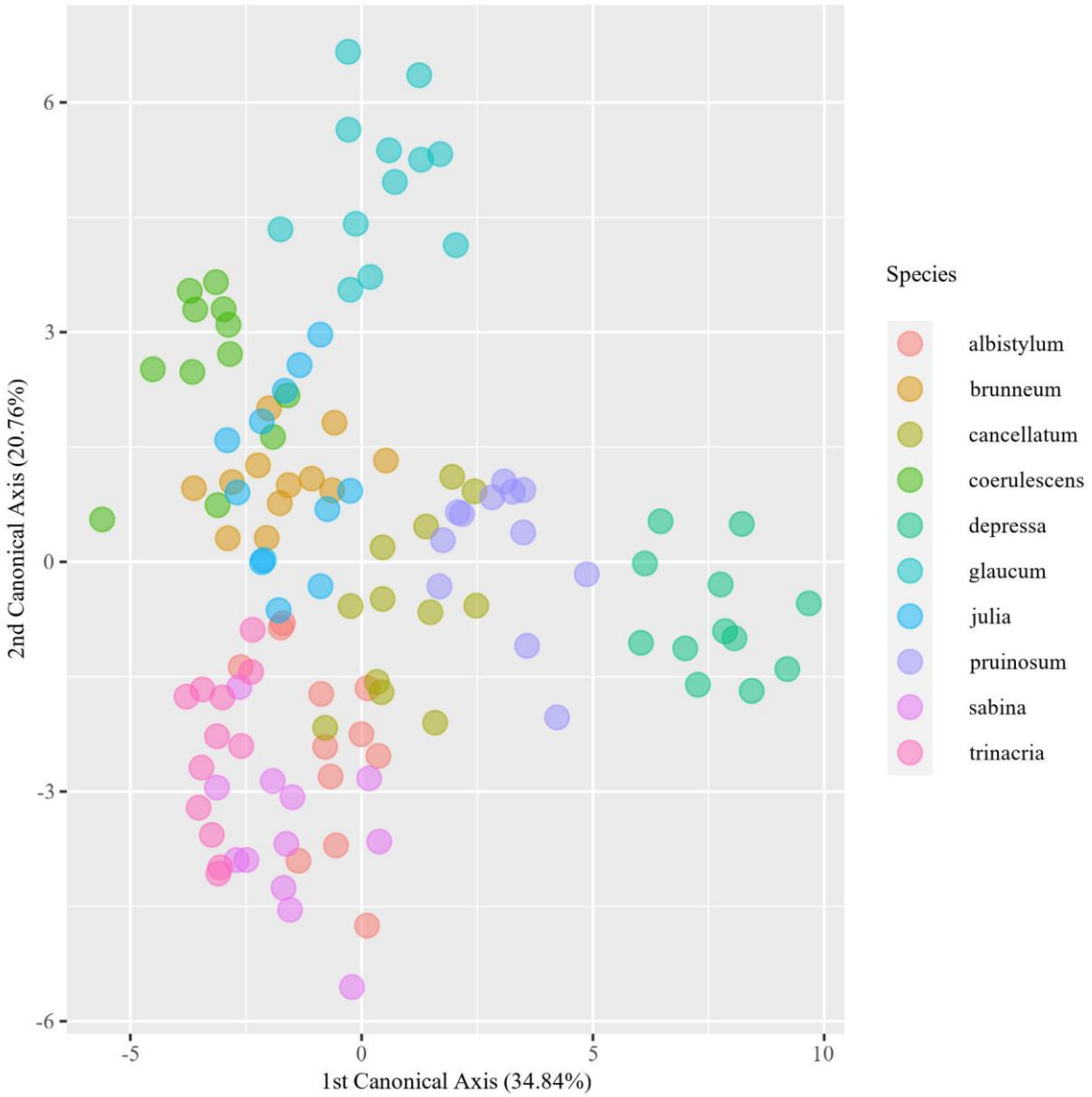

Figure 5. Canonical Variate Analysis (CVA) score plot of hindwing shape in *Orthetrum* (+ *Libellula depressa*), based on landmark coordinates after Generalized Procrustes Analysis. Individuals are grouped according to predefined species, highlighting patterns of interspecific shape differentiation.

reflecting some overlap in hindwing shape. The test ran on pairwise Mahalanobis distances returned statistically significant differences in hindwing shape among most *Orthetrum* species ($p < 0.01$). Linear discriminant analysis (LDA) was also performed for the hindwing data to assess sexual differences in hindwing shape. Cross-validated classification correctly assigned 73.3% of individuals to their sex, with a Cohen's κ of 0.46, indicating only a moderate discriminative power. Classification was slightly less accurate for females (73.1%) than for males (73.5%).

Table 6. Cross-validated classification matrix (%) obtained from Canonical Variate Analysis (CVA) of Procrustes-aligned hindwing landmark data. Species abbreviations: alb (*albistylum*), bru (*brunneum*), can (*cancellatum*), coe (*coerulescens*), dep (*depressa*), gla (*glaucum*), jul (*julia*), pru (*pruinosum*), sab (*sabina*), tri (*trinacria*).

	alb	**bru**	**can**	**coe**	**dep**	**gla**	**jul**	**pru**	**sab**	**tri**
alb	50.00	25.00	8.33	0.00	0.00	0.00	0.00	0.00	16.67	0.00
bru	8.33	66.67	8.33	0.00	0.00	0.00	16.67	0.00	0.00	0.00
can	16.67	8.33	66.67	0.00	0.00	0.00	0.00	8.33	0.00	0.00
coe	0.00	25.00	0.00	75.00	0.00	0.00	0.00	0.00	0.00	0.00
dep	0.00	0.00	0.00	0.00	100.00	0.00	0.00	0.00	0.00	0.00
gla	0.00	0.00	8.33	0.00	0.00	66.67	16.67	8.33	0.00	0.00
jul	0.00	8.33	0.00	0.00	0.00	0.00	75.00	0.00	0.00	16.67
pru	0.00	0.00	8.33	0.00	8.33	0.00	8.33	75.00	0.00	0.00
sab	0.00	0.00	0.00	0.00	0.00	0.00	0.00	0.00	100.00	0.00
tri	0.00	0.00	0.00	0.00	0.00	0.00	8.33	0.00	0.00	91.67

DISCUSSION

The primary aim of this study was to provide a quantitative, landmark-based assessment of wing shape variation in a representative subset of *Orthetrum* species, with a particular focus on evaluating the methodological and taxonomic information content of wing morphology. By explicitly addressing interspecific variation, intraspecific variability, sexual dimorphism, and the reliability of community-sourced image data, the results offer a structured framework for interpreting wing shape as a morphological character within the genus. The analyses clearly demonstrate that wing shape contains a consistent interspecific signal across the examined *Orthetrum* species, although the strength and structure of this signal differ between forewings and hindwings. Multivariate analyses (PCA and CVA) reveal that hindwing morphology captures interspecific differences more effectively than forewing morphology, as evidenced by stronger separation in morphospace, higher proportions of variance concentrated in the first principal components, and largely significant pairwise Mahalanobis distances (Blanke, 2018; Huang et al., 2020). These results indicate that hindwing shape variation is organized along a limited number of dominant axes that are particularly informative for distinguishing species. In contrast, forewing shape exhibits greater overlap among taxa and a more diffuse distribution of variance across principal components. Although most species pairs remain statistically distinguishable, classification accuracy is reduced for several taxa, and misclassification patterns indicate partial shape similarity among closely related or morphologically similar species. These results together indicate that hindwings provide a more robust and structured interspecific signal than forewings when analysed using geometric morphometric approaches as already observed by Gayathr et al. (2023) for *Pantala flavescens*. Previous studies in Odonata have suggested that wing morphology may covary with behavioural traits such as flight or perching style (Grabow & Rüppel, 1995; Sacchi & Hardersen, 2013). While our study does not test these associations directly, some of the interspecific variation observed here may partially reflect such species-specific factors. Regardless of these potential influences, our results demonstrate that landmark-based geometric morphometrics captures consistent interspecific differences that can be used as a complementary tool for taxonomic identification. A focal point of this study was to assess the magnitude of

intraspecific variation relative to interspecific divergence to evaluate the taxonomic resolution achievable through wing shape analysis. The observed overlap among species in PCA and CVA space - particularly for forewings and for specific species pairs in hindwings - demonstrates that intraspecific variability is non-negligible and can partially hide species boundaries in morphometric space. Despite this overlap, interspecific differences generally exceed intraspecific variation, especially in hindwing morphology.

The broader geographic coverage of this study may have captured variation among populations, as observed in other taxa of this order (Hassall, 2009; Sadeghi, 2014) which, while representing normal intraspecific variation, can also contribute an additional source of uncertainty

However, the persistence of statistically significant pairwise Mahalanobis distances among most species pairs indicates that wing shape retains a certain discriminatory power even when intraspecific variability is taken into account. These results support the use of wing shape as a quantitative descriptor of morphological differentiation, while emphasizing that species discrimination based on morphometrics should be interpreted probabilistically rather than as an absolute diagnostic criterion. Sexual shape dimorphism was detected consistently in both forewings and hindwings, although its magnitude was modest relative to interspecific differentiation. PCA, CVA, and discriminant analyses indicate that males and females differ significantly in wing shape, but with substantial overlap in morphospace and moderate classification accuracy. This pattern indicates that sexual dimorphism contributes to overall shape variation without dominating the multivariate structure of the data. From a methodological perspective, the limited magnitude of sexual dimorphism has two important implications. First, it suggests that pooling sexes in interspecific analyses does not artificially inflate species-level differentiation. Second, it indicates that wing shape can be used in taxonomic contexts without requiring strict sex-specific datasets, provided that sex is considered analytically. Sexual dimorphism therefore represents a secondary but detectable source of variation within the broader morphometric framework. Allometric analyses clarify the role of size in shaping wing morphology and its contribution to interspecific differentiation. In both wing pairs, species-specific allometric trajectories were supported statistically as already described in Eshghi et al. (2024); however, pairwise comparisons reveal that interspecific differences in the magnitude of allometric change are generally limited. In forewings, species differ primarily in the orientation of allometric trajectories, whereas differences in the rate of shape change with size are small. Hindwings, by contrast, exhibit a largely conserved allometric pattern across species, with minimal interspecific divergence in both trajectory magnitude and direction. Importantly, removal of the allometric component does not alter the main interspecific structure observed in PCA and CVA analyses for either wing pair. This demonstrates that species separation in morphometric space is not an artifact of size variation and that the primary interspecific signal in wing shape is largely size-independent. Allometry therefore modulates the expression of shape variation without driving the main patterns of species differentiation. Although centroid size differs significantly among species, these results indicate that shape variation captures patterns of morphological differentiation that are not reducible to size alone. In this context, the shape of flight-related structures, rather than their linear dimensions, provides a more integrative description of interspecific morphological differences when size-related effects are explicitly accounted for (Suárez-Tovar & Sarmiento, 2016; Outomuro et al., 2013). A further objective of this study was

to test the feasibility and reliability of using digital images sourced from iNaturalist and other online repositories for geometric morphometric analyses. The results demonstrate that, despite heterogeneity in image resolution, orientation, and background, community-generated images can reliably capture biologically meaningful wing shape variation. The detection of consistent interspecific and sexual differences using these data supports their suitability for large-scale comparative morphometric studies and enables substantially broader sampling than traditional specimen-based approaches. The consistent interspecific signal detected - particularly in hindwing morphology - demonstrates that geometric morphometrics provides a valuable complementary line of evidence. Wing shape analysis is especially useful for quantifying morphological similarity, identifying cases of partial overlap, and supporting integrative taxonomic frameworks. Overall, this study highlights the methodological utility of landmark-based geometric morphometrics for assessing wing shape variation in *Orthetrum*. By explicitly quantifying interspecific divergence, intraspecific variability, sexual dimorphism, and size effects, and by validating the use of online image repositories, the results provide a clear and reproducible framework for future taxonomically oriented morphometric studies in Odonata. From a taxonomic perspective, wing morphology - particularly when quantified using landmark-based geometric morphometrics. provides a valuable complementary tool for species discrimination. While genital morphology and other traditional diagnostic characters remain the primary basis for species identification, the consistent interspecific signal detected in hindwing and, to a lesser extent, forewing shape demonstrates that wings can enhance taxonomic resolution. This is especially relevant in challenging cases, such as cryptic species pairs, closely related taxa with partial overlap of form, or damaged specimens, where landmark-based analyses reveal consistent and informative patterns, for example in the forewing radial region and hindwing lobes. Applying standardized morphometric protocols ensures reproducibility across specimens, including those sourced from community-generated image repositories, and supports integrative taxonomic frameworks by providing quantitative evidence that complements traditional characters.

Wing morphology, quantified through landmark-based geometric morphometrics, may provide a valuable tool for the taxonomy of genus *Orthetrum*, as already demonstrated for other Libellulidae (Tarrís-Samaniego, 2013), particularly in cases where molecular phylogenetic analyses do not fully resolve relationships among closely related species (Yong et al., 2014). While genital morphology and other established diagnostic traits remain primary, wing shape can reveal consistent interspecific differences even among cryptic or morphologically similar species (Johansson et al., 2009), or in damaged specimens where traditional characters are incomplete. By applying standardized morphometric protocols, including analyses of community-sourced images, wings can reliably complement traditional characters and molecular data, supporting integrative identification frameworks and enhancing reproducibility across specimens.

CONCLUSIONS

Taken together, these results indicate that wing morphology in *Orthetrum* may reflect a combination of conserved functional constraints, species-specific ecological adaptation, and subtle sexual dimorphism. The coexistence of shared and divergent allometric trajectories suggests a balance between species-specific shape differentiation and the maintenance of functional integrity. Multivariate patterns revealed by PCA and CVA underpin that hindwing

shape provides a particularly strong signal for species differentiation, whereas forewing morphology, although informative, may be less reliable for discriminating closely related taxa. The observed patterns of shape variation are consistent with multiple, potentially interacting drivers. Wing shape variation appears to be structured along consistent morphological gradients, particularly in the hindwings, where differences in width and outline contribute to interspecific separation. At the same time, similarities in overall wing architecture among some taxa suggest the retention of shared morphological patterns, potentially reflecting common ancestry rather than independent shape convergence. Allometric analyses indicate that species-specific size-shape relationships modulate, but do not drive the primary patterns of shape divergence. Sexual dimorphism is detectable but secondary relative to interspecific differences. Importantly, the use of community-sourced digital images proved effective for capturing biologically meaningful variation, highlighting the feasibility of large-scale morphometric analyses without reliance on traditional specimen collections. Overall, these findings underscore the utility of geometric morphometrics for standardizing wing shape analyses and providing complementary evidence in taxonomic studies of Odonata.

AKNOWLEDGEMENTS - We would like to thank Dr Daniele Baroni for his critical review and valuable suggestions on the text.

REFERENCES

Adams D.C., Rohlf F.J. & Slice D.E., 2004. Geometric morphometrics: ten years of progress following the 'revolution'. Italian Journal of Zoology 71(1): 5-16. https://doi.org/10.1080/11250000409356545

Baken E.K., Collyer M.L., Kaliontzopoulou A. & Adams D.C., 2021. geomorph v4. 0 and gmShiny: Enhanced analytics and a new graphical interface for a comprehensive morphometric experience. Methods in Ecology and Evolution 12(12): 2355-2363. https://doi.org/10.1111/2041-210X.13723

Blanke A., 2018. Analysis of modularity and integration suggests evolution of dragonfly wing venation mainly in response to functional demands. Journal of the Royal Society Interface 15(145): 20180277. https://doi.org/10.1098/rsif.2018.0277

Bookstein F.L.,1997. Morphometric tools for landmark data.

Cardini A., de Jong Y.A. & Butynski T.M., 2022. Can morphotaxa be assessed with photographs? Estimating the accuracy of two-dimensional cranial geometric morphometrics for the study of threatened populations of African monkeys. The Anatomical Record 305(6): 1402-1434. https://doi.org/10.1002/ar.24787

Collyer M.L. & Adams D.C., 2018. RRPP: An r package for fitting linear models to high-dimensional data using residual randomization. Methods in Ecology and Evolution 9(7): 1772-1779. https://doi.org/10.1111/2041-210X.13029

Corbet P.S., 1999. Dragonflies: Behavior and Ecology of Odonata. Cornell University Press.

Dijkstra K.-D.B. & Kalkman V.J., 2012. Phylogeny, classification and taxonomy of European dragonflies and damselflies (Odonata): a review. Organisms Diversity & Evolution 12: 209–227.

Dijkstra K.-D.B., Bechly G., Bybee S.M., Dow R.A., Dumont H.J., Fleck G., Garrison R.W., Hämäläinen M., Kalkman V.J., … Ware J., 2013. The classification and diversity of dragonflies and damselflies (Odonata). In: Zhang Z.-Q. (ed.), Animal Biodiversity: An Outline of Higher-level Classification and Survey of Taxonomic Richness. Zootaxa 3703: 36-45. https://doi.org/10.11646/zootaxa.3703.1.9

Dryden I.L., Mardia K.V. 1998. Statistical shape analysis. Wiley, Chichester, xvii+347 pp.

Dumont H.J., Vierstraete A. & Vanfleteren J.R., 2010. A molecular phylogeny of the Odonata (Insecta). Systematic Entomology 35: 6-18.

Eshghi S., Rajabi H., Shafaghi S., Nabati F., Nazerian S., Darvizeh A. & Gorb S.N., 2024. Allometric

scaling reveals evolutionary constraint on Odonata wing cellularity via critical crack length. Advanced Science 11(23): 2400844. https://doi.org/10.1002/advs.202400844

Fox N.S., Veneracion J.J. & Blois J.L., 2020. Are geometric morphometric analyses replicable? Evaluating landmark measurement error and its impact on extant and fossil *Microtus* classification. Ecology and evolution 10(7): 3260-3275. https://doi.org/10.1002/ece3.6063

Gayathri M., Anand P.P. & Shibu Vardhanan Y., 2023. Wing size, shape, and asymmetry analysis of the wandering glider, *Pantala flavescens* (Odonata: Libellulidae) revealed that hindwings are more asymmetric than the forewings. Biologia 78(10): 2749-2762. https://doi.org/10.1007/s11756-023-01396-5

Gower J.C., 1975. Generalized procrustes analysis. Psychometrika 40(1): 33-51.

Grabow, K., & Rüppell, G., 1995. Wing loading in relation to size and flight characteristics of European Odonata. Odonatologica 24(2): 175-186.

Gumiel M., Catalá S., Noireau F., Rojas de Arias A., Garcia A. & Dujardin J.P., 2003. Wing geometry in *Triatoma infestans* (Klug) and *T. melanosoma* Martinez, Olmedo & Carcavallo (Hemiptera: Reduviidae). Systematic Entomology 28(2): 173-180. https://doi.org/10.1046/j.1365-3113.2003.00206

Hassall C., 2015. Strong geographical variation in wing aspect ratio of a damselfly, *Calopteryx maculata* (Odonata: Zygoptera). PeerJ 3: e1219. https://doi.org/10.7717/peerj.1219

Hebert P.D.N., Cywinska A., Ball S.L. & deWaard J.R., 2003. Biological identifications through DNA barcodes. Proceedings of the Royal Society B 270: 313-321.

Huang S.-T., Wang H.-R., Yang W.-Q., Si Y.-C., Wang Y.-T., Sun M.-L., Qi X. & Bai Y., 2020. Phylogeny of Libellulidae (Odonata: Anisoptera): comparison of molecular- and morphology-based phylogenies based on wing morphology and migration. PeerJ 8: e8567. https://doi.org/10.7717/peerj.8567

Johansson F., Söderquist M. & Bokma F., 2009. Insect wing shape evolution: independent effects of migratory and mate guarding flight on dragonfly wings. Biological journal of the Linnean Society 97(2): 362-372.

Klingenberg C.P. & McIntyre G.S, 1998. Geometric morphometrics of developmental instability: analyzing patterns of fluctuating asymmetry with Procrustes methods. Evolution 52(5): 1363-1375. https://doi.org/10.1111/j.1558-5646.1998.tb02018

Klingenberg C.P. & Zaklan S.D., 2000. Morphological integration between developmental compartments in the Drosophila wing. Evolution 54(4): 1273-1285. https://doi.org/10.1111/j.0014-3820.2000.tb00560.x

Marinov M., 2001. The *Orthetrum coerulescens* complex in Bulgaria (Odonata: Libellulidae). International Journal of Odonatology 4(1): 35-40. https://doi.org/10.1080/13887890.2001.9748156

Mason B.M., Mesaglio T., Heitmann J.B., Chandler M., Chowdhury S., Gorta S.B.Z., Grattarola F., Groom Q., Hitchcock C., ... Callaghan C.T., 2025. iNaturalist accelerates biodiversity research. BioScience 75(11): 953–965. https://doi.org/10.1093/biosci/biaf104

Outomuro D., Adams D.C. & Johansson F., 2013. The evolution of wing shape in ornamented-winged damselflies (Calopterygidae, Odonata). Evolutionary Biology 40: 300-309. https://doi.org/10.1007/s11692-012-9214-3

Outomuro D. & Johansson F., 2011. The effects of latitude, body size, and sexual selection on wing shape in a damselfly. Biological Journal of the Linnean Society 102: 263–274.

Ripley B., Venables B., Bates D.M., Hornik K., Gebhardt A., Firth D. & Ripley M.B., 2013. *Package MASS*. CRAN, Vienna.

Rohlf F.J., 1999. Shape statistics: Procrustes superimpositions and tangent spaces. Journal of classification 16(2): 197-223. https://doi.org/10.1007/s003579900054

Rohlf F.J., 2017a. tpsUtil32. New York: Department of Ecology and Evolution, State University of New York at Stony Brook. Available at http://life.bio.sunysb.edu/morph/

Rohlf F.J., 2017b. TpsDig, version 2.30. New York: Department of Ecology and Evolution, State University of New York at Stony Brook. Available at http://life.bio.sunysb.edu/morph/

Rohlf F.J. & Slice D. 1990. Extensions of the Procrustes method for the optimal superimposition of landmarks. Systematic Biology 39(1): 40-59. https://doi.org/10.2307/2992207

Sacchi R. & Hardersen S., 2013. Wing length allometry in Odonata: differences between families in relation to migratory behaviour. Zoomorphology 132: 23-32. https://doi.org/10.1007/s00435-012-0172-1

Sadeghi S., 2014. Variation in the shape of the wings and taxonomy of Eurasian populations of the *Calopteryx splendens* complex (Odonata: Calopterygidae). European Journal of Entomology

111(4): 575-583. https://doi.org/10.14411/EJE.2014.073
Schlager S., Jefferis G., Ian D. & Schlager M.S., 2019. *Morpho*: R package for geometric morphometrics.
Silsby J., 2001. Dragonflies of the World. Smithsonian Institution Press.
Suárez-Tovar, C.M. & Sarmiento C.E., 2016. Beyond the wing planform: morphological differentiation between migratory and nonmigratory dragonfly species. Journal of Evolutionary Biology 29(4): 690-703. https://doi.org/10.1111/jeb.12830
Tarrís-Samaniego S., Muzón J. & Iglesias M.S., 2023. When size and shape matter: morphometric characterization of two sympatric dragonflies of the genus *Perithemis* (Odonata: Libellulidae). Anais da Academia Brasileira de Ciências 95(suppl 1): e20220583. https://doi.org/10.1590/0001-3765202320220583
Villemant C., Simbolotti G. & Kenis M., 2007. Discrimination of *Eubazus* (Hymenoptera, Braconidae) sibling species using geometric morphometrics analysis of wing venation. Systematic Entomology 32(4): 625-634. https://doi.org/10.1111/j.1365-3113.2007.00389.x
Wootton R.J., 1991. The functional morphology of the wings of Odonata. Advances in odonatology 5(1): 153-169.
Yong H.S., Lim P.E., Tan J., Ng Y.F., Eamsobhana P. & Suana I.W., 2014. Molecular phylogeny of *Orthetrum* dragonflies reveals cryptic species of *Orthetrum pruinosum*. Scientific Reports 4(1): 5553. https://doi.org/10.1038/srep0555
Zelditch M., Swiderski D. & Sheets H.D., 2012. Geometric morphometrics for biologists: a primer. Academic press.

DOI: 10.15167/2612-2960/BELS2025.7.1.2718